

**The *Mycobacterium abscessus* cytochrome *bcc:aa₃* oxidase structure paves the way
for an agent targeting subunit QcrB**

Vikneswaran Mathiyazakan¹, Emilia Tan Xin Yi¹, Garrett C. Moraski², Sandip Basak^{1,3},
Wuan-Geok Saw³, Kevin Pethe⁴⁻⁷ and Gerhard Grüber^{1*}

Supplementary Information

Supplementary Figure 1-9

Supplementary Tables 1-10

General synthesis routes to compounds

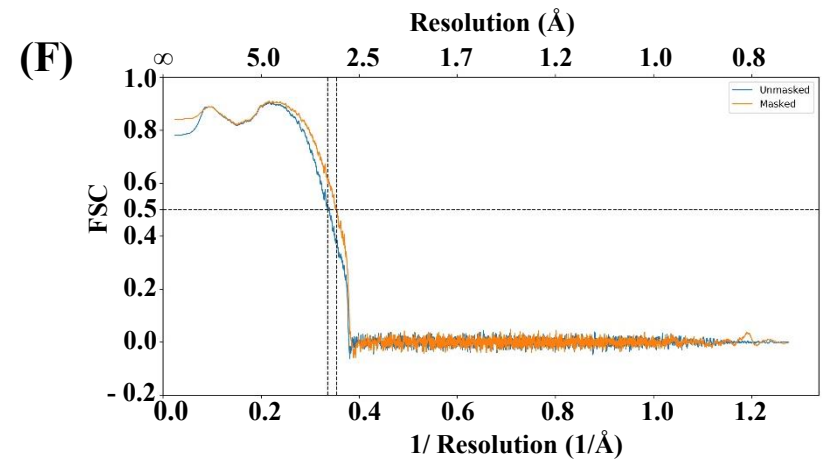
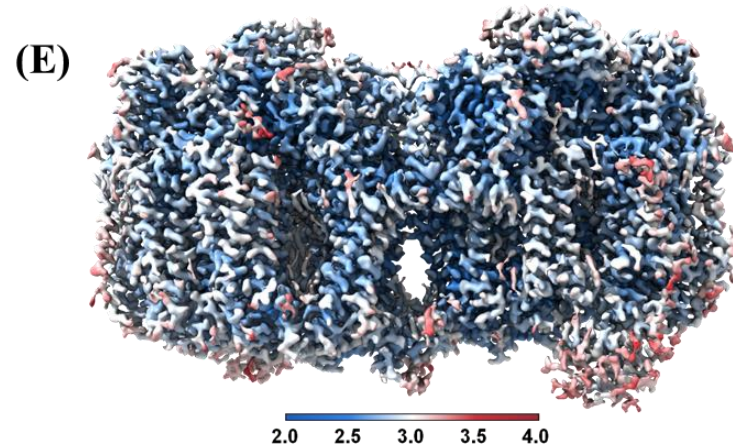
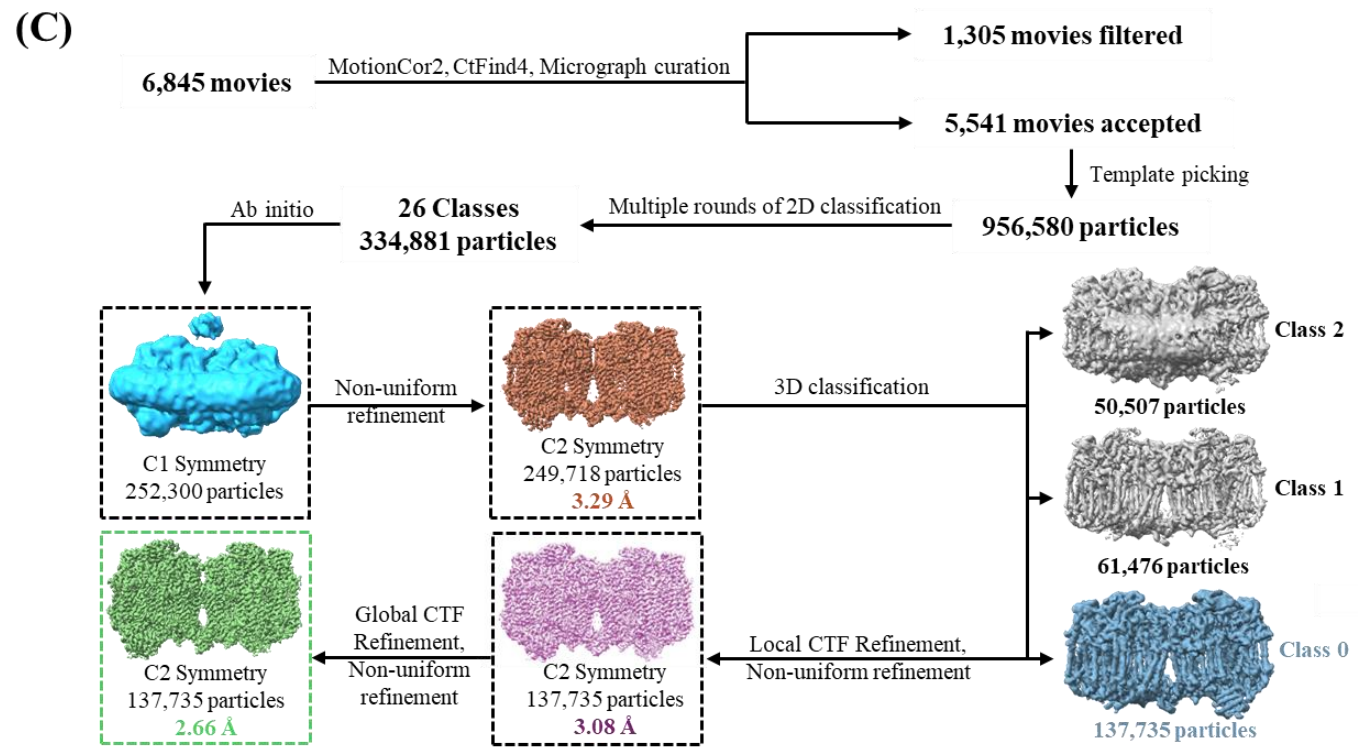
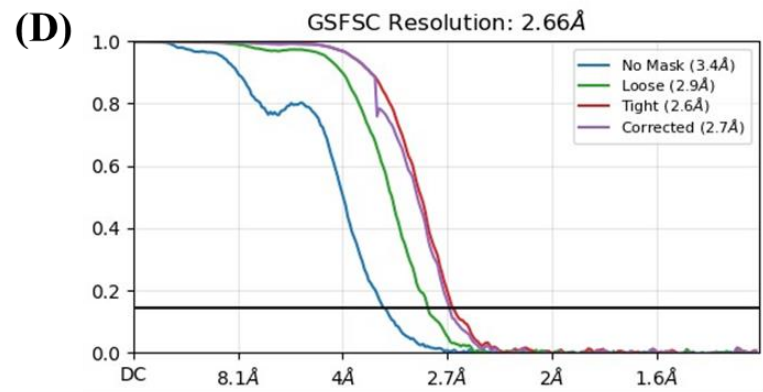
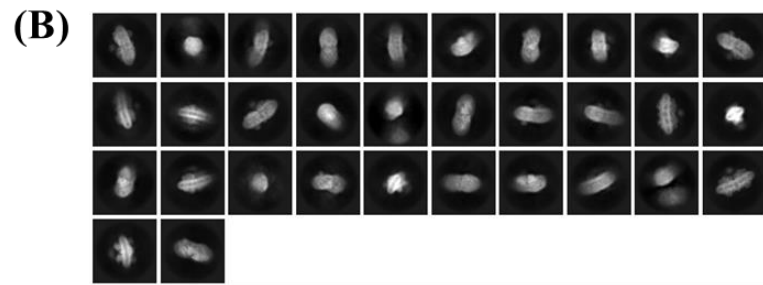
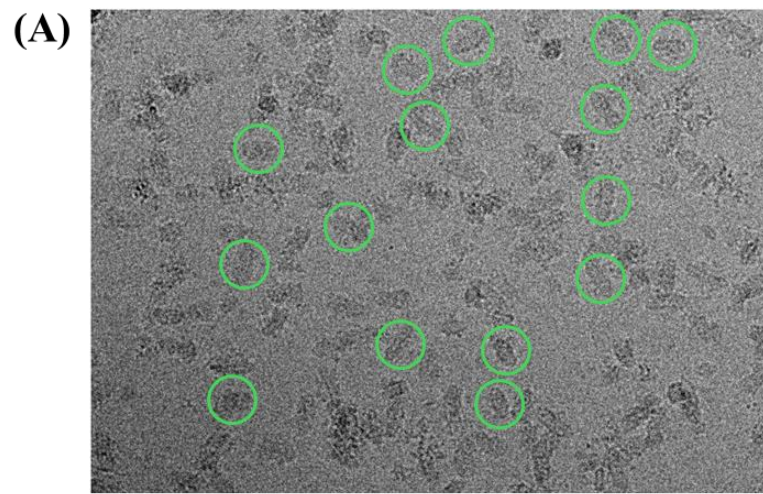
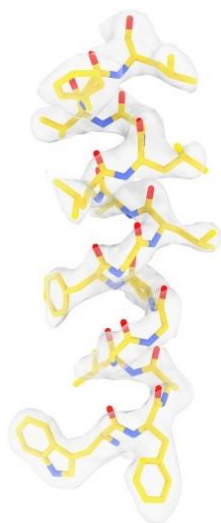


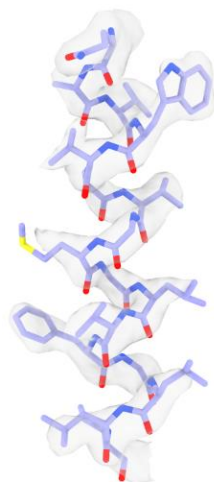
*Figure legend in next page

Supplementary Figure 1. Cryo-EM workflow. (A) Identification of *M. abscessus* cyt-*bcc:aa*₃ particles in grid screening. (B) 2D-classification of picked particles in CryoSPARC. (C) Cryo-EM data processing workflow. The data processing pipeline was performed in cryoSPARC v3.3.1. 6,845 movies were collected and subjected to motion correction (MotionCor2) and CTF estimation (CtFind4). The processed micrographs were subsequently curated with the following thresholds: CTF fit resolution Min: 3.97 Å; Max: 7 Å and Astigmatism Min: 0.47 Å; Max: 500 Å resulting in the acceptance of 5,541 exposures for downstream processing. The *M. smegmatis* cyt-*bcc:aa*₃ oxidase structure (PDB: 6ADQ) was imported into cryoSPARC and used to generate templates for template-based picking yielding 956,580 particles. The particles were binned by a factor of 4 during the particle extraction process to reduce computational time and subjected to multiple rounds of 2D classification. 26 classes containing 334,881 particles were selected to construct an ab initio model with C1 symmetry. The ab initio model accepted 252,300 particles which were then reextracted at full resolution and subjected to non-uniform refinement resulting in a refined map with 249,718 particles with an overall resolution of 3.29 Å. A 3D classification job was performed to classify the particle into 3 classes using C1 symmetry. Class 0 emerged as the largest class with 137,735 particles which was then subjected to local CTF refinement followed by non-uniform refinement. The resulting map, which had an overall resolution of 3.08 Å, was refined further using global CTF refinement and another round of non-uniform refinement yielding a final cryo-EM map with an overall resolution of 3.29 Å with 137,735 particles. (D) Data processing in CryoSPARC and Relion resulted in a *M. abscessus* cyt-*bcc:aa*₃ structure at 2.66 Å. (E) Local resolution gradient map (2.0 Å, Blue; 4.0 Å, Red) reveals high resolution in core and key reaction centers. (F) Map vs Model FSC curve.

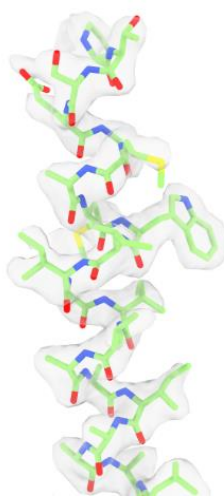
Mab cyt-bcc



QcrA ₆₂₋₇₈

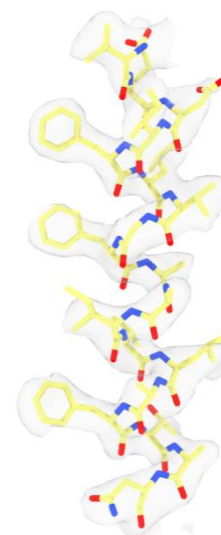


QcrB ₃₃₁₋₃₄₇

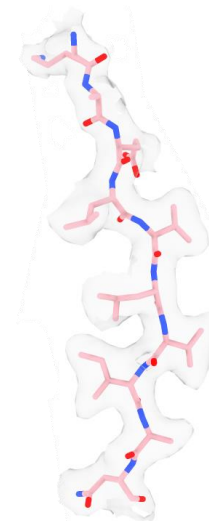


QcrC ₂₆₉₋₂₉₀

Accessory units

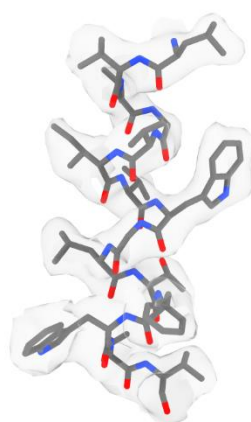


PRSAF ₅₇₋₇₅

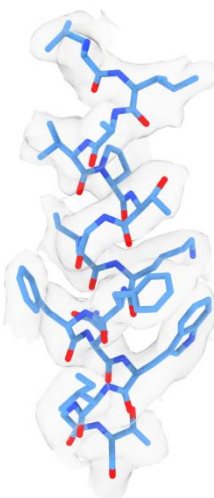


LpqE ₇₅₋₈₄

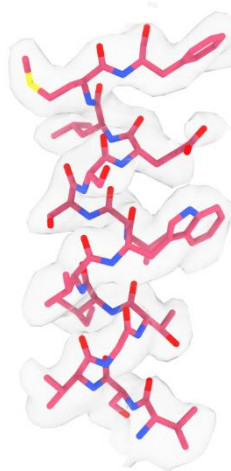
Mab cyt-aa₃



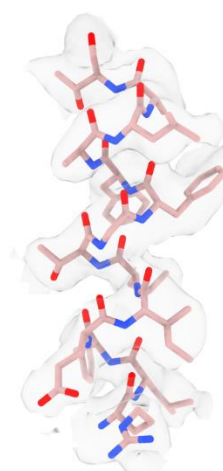
CtaC ₆₂₋₇₆



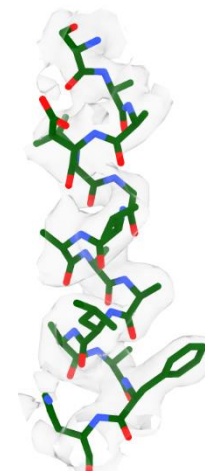
CtaD ₃₃₂₋₃₄₇



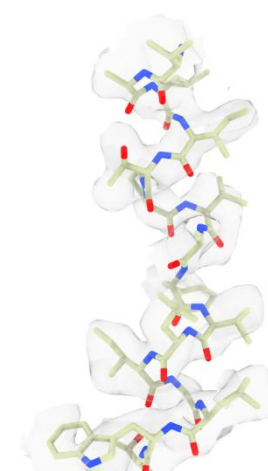
CtaE ₂₈₋₄₂



CtaF ₆₋₁₉

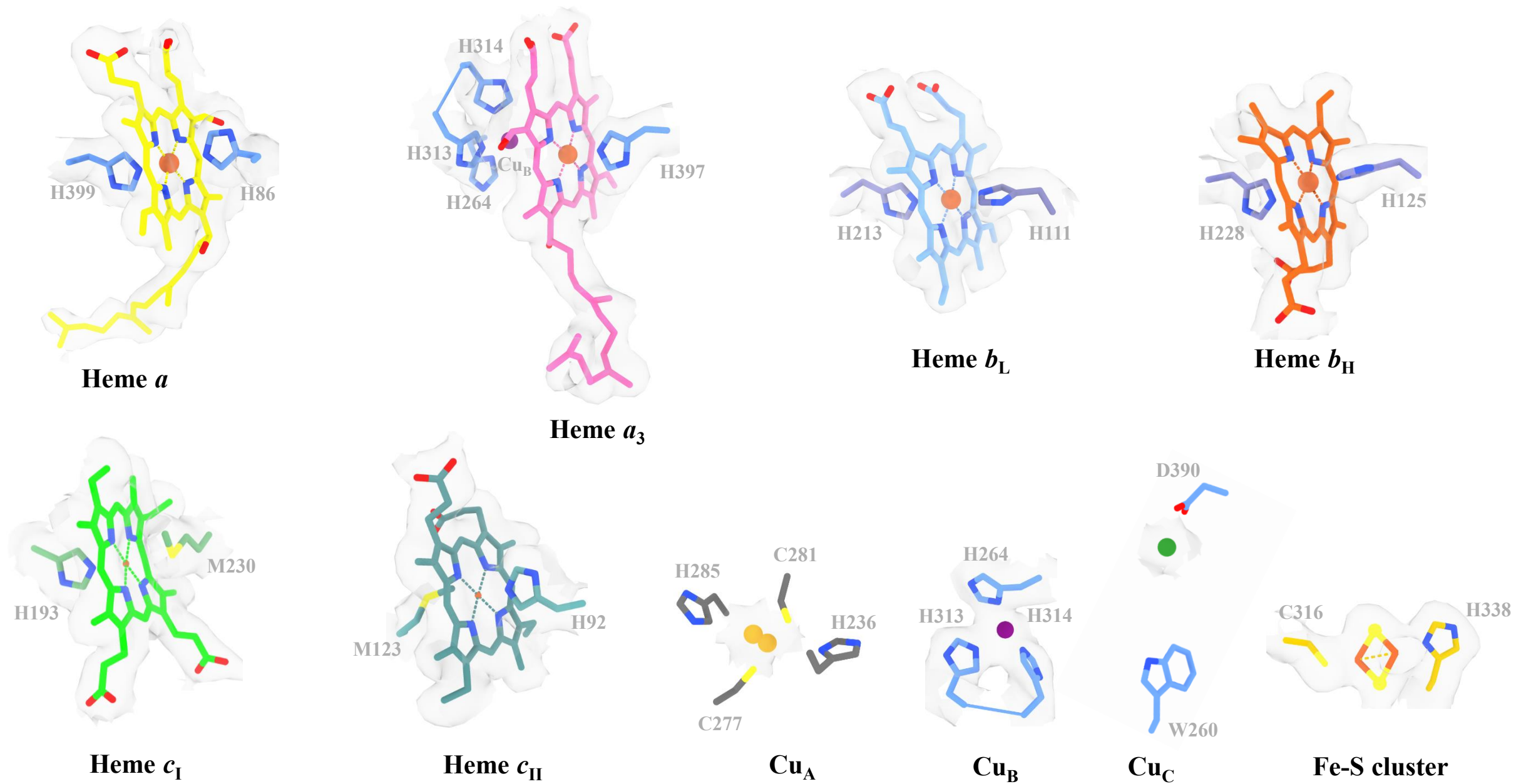


CtaI ₁₃₉₋₁₅₃

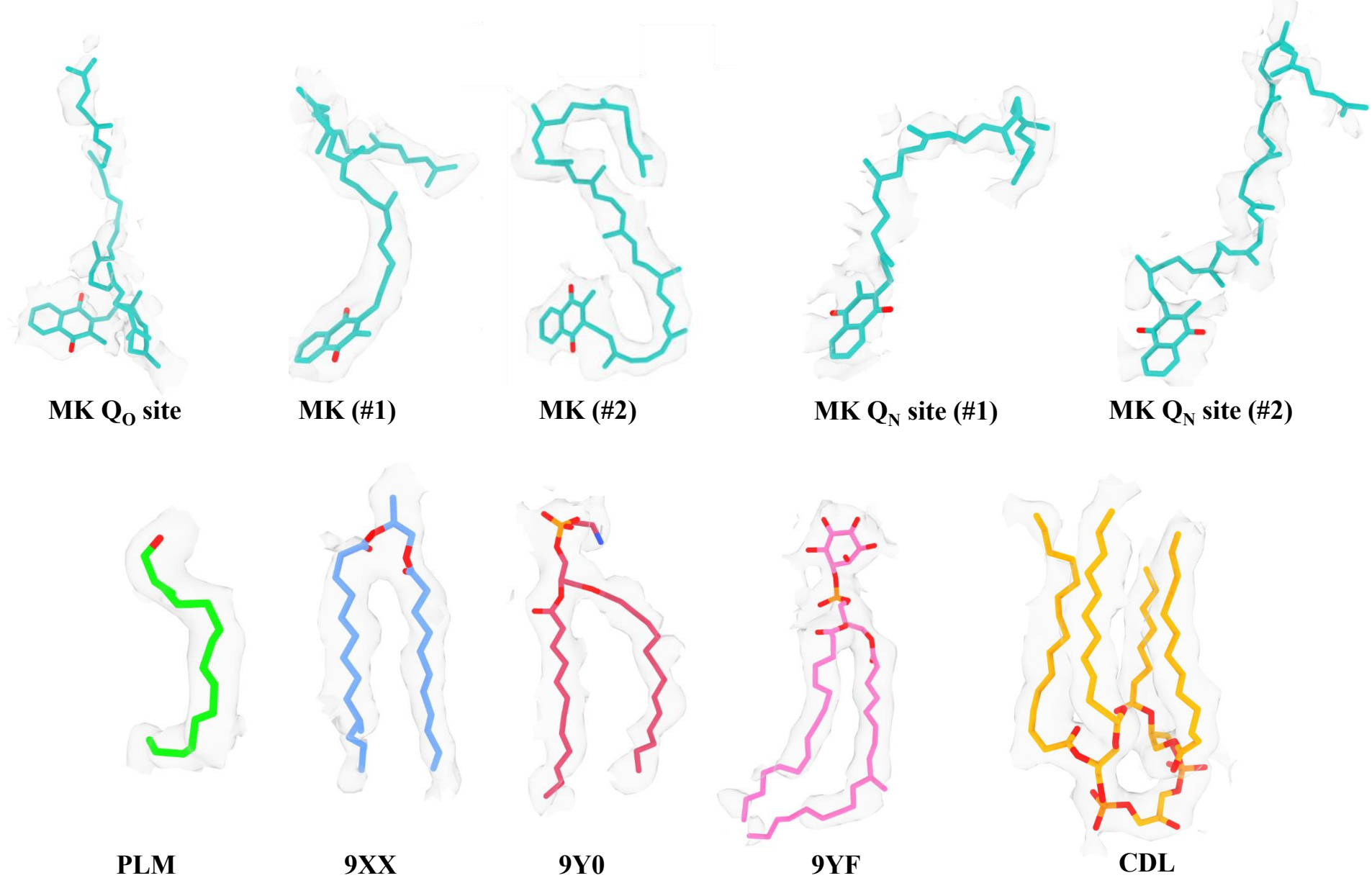


CtaJ ₁₆₋₃₁

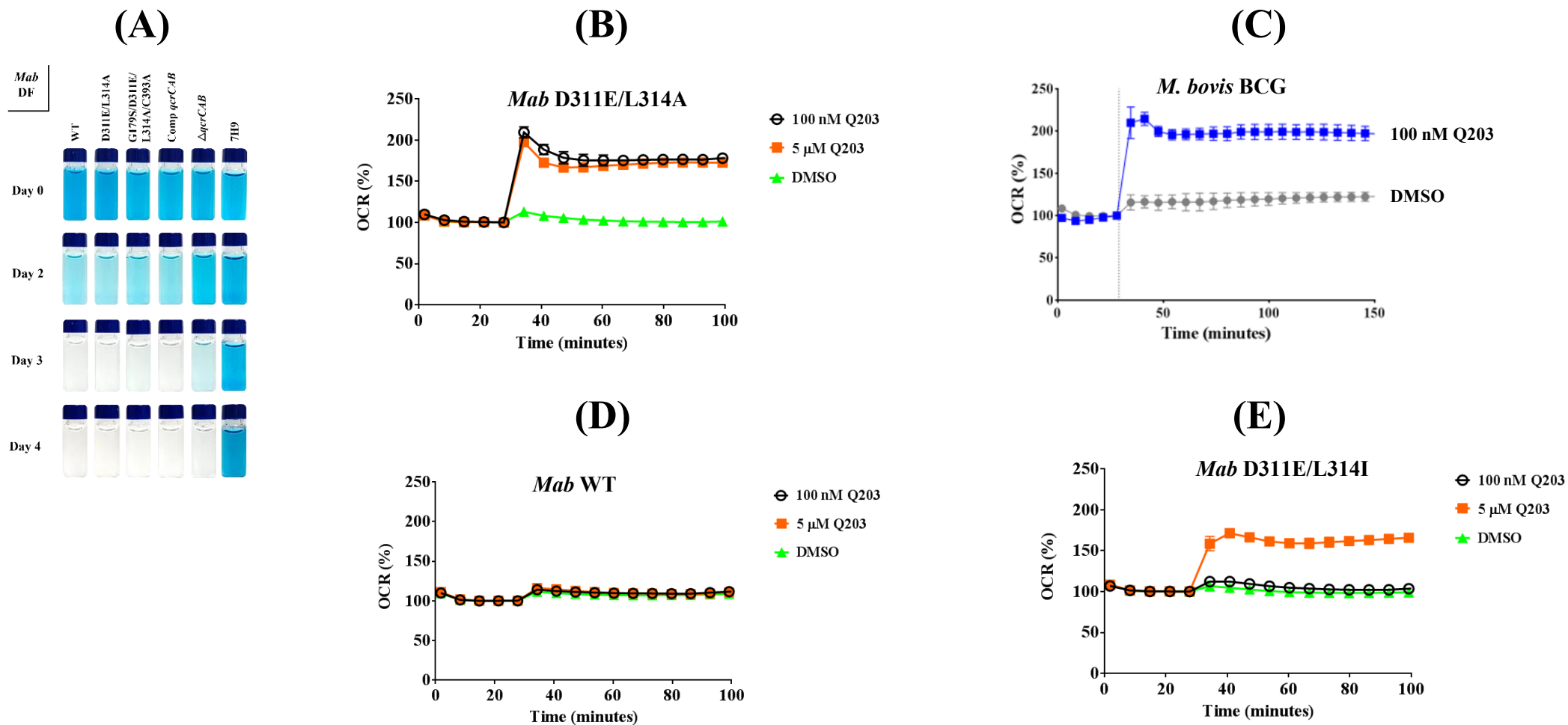
Supplementary Figure 2. Cryo-EM density maps of the *M. abscessus* cyt-*bcc:aa₃* supercomplex structural and accessory units. The density maps were visualized using ChimeraX (Step:1, Contour level: 0.326).



Supplementary Figure 3. Cryo-EM density maps of the *M. abscessus* *cyt-bcc:aa₃* regulatory elements. The density maps were visualized using ChimeraX (Step:1, Contour level: 0.326).



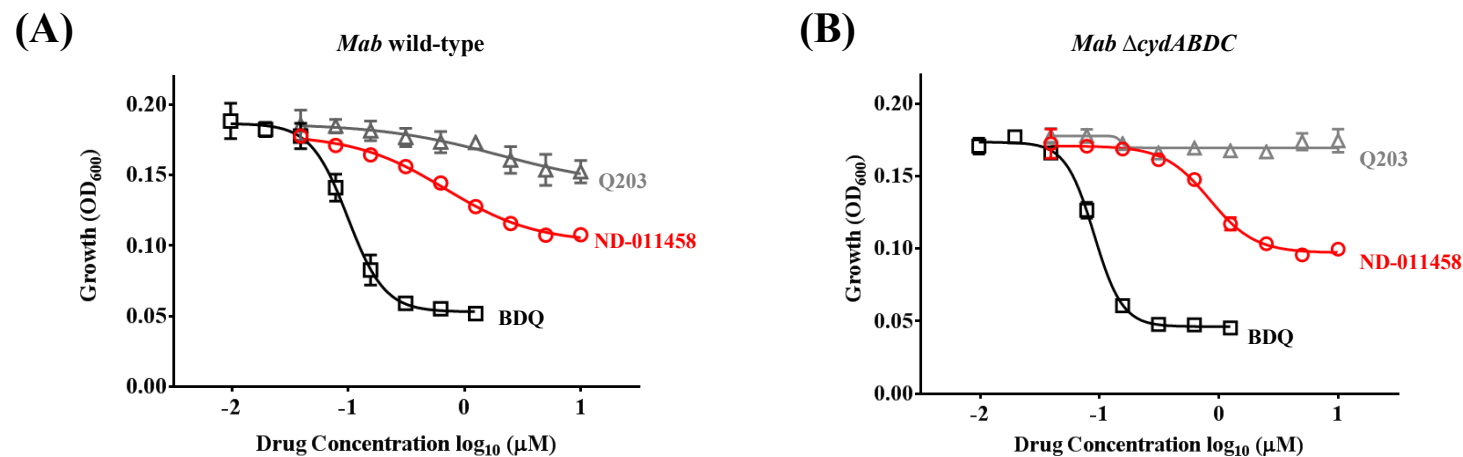
Supplementary Figure 4. Cryo-EM density maps of the *M. abscessus* *cyt-bcc:aa₃* ligands and lipids. The density maps were visualized using ChimeraX (Step:1, Contour level: 0.326).



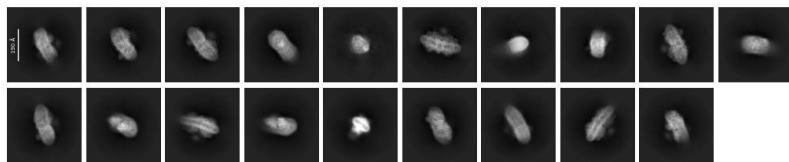
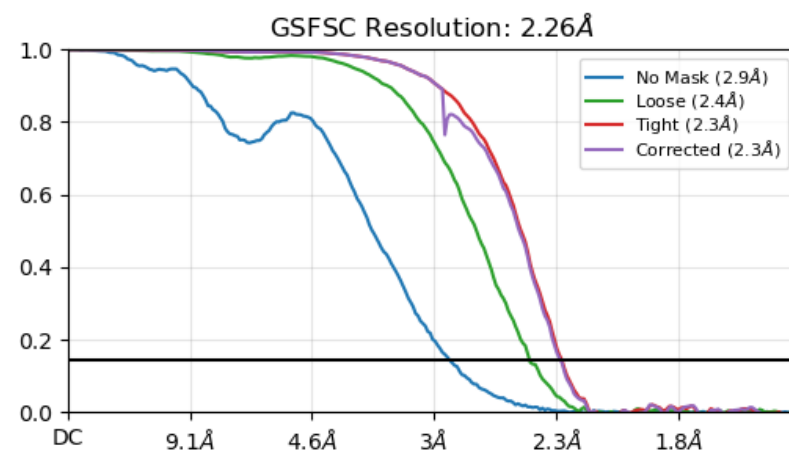
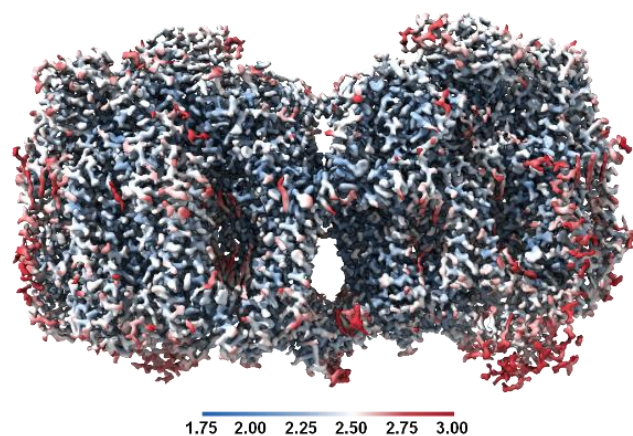
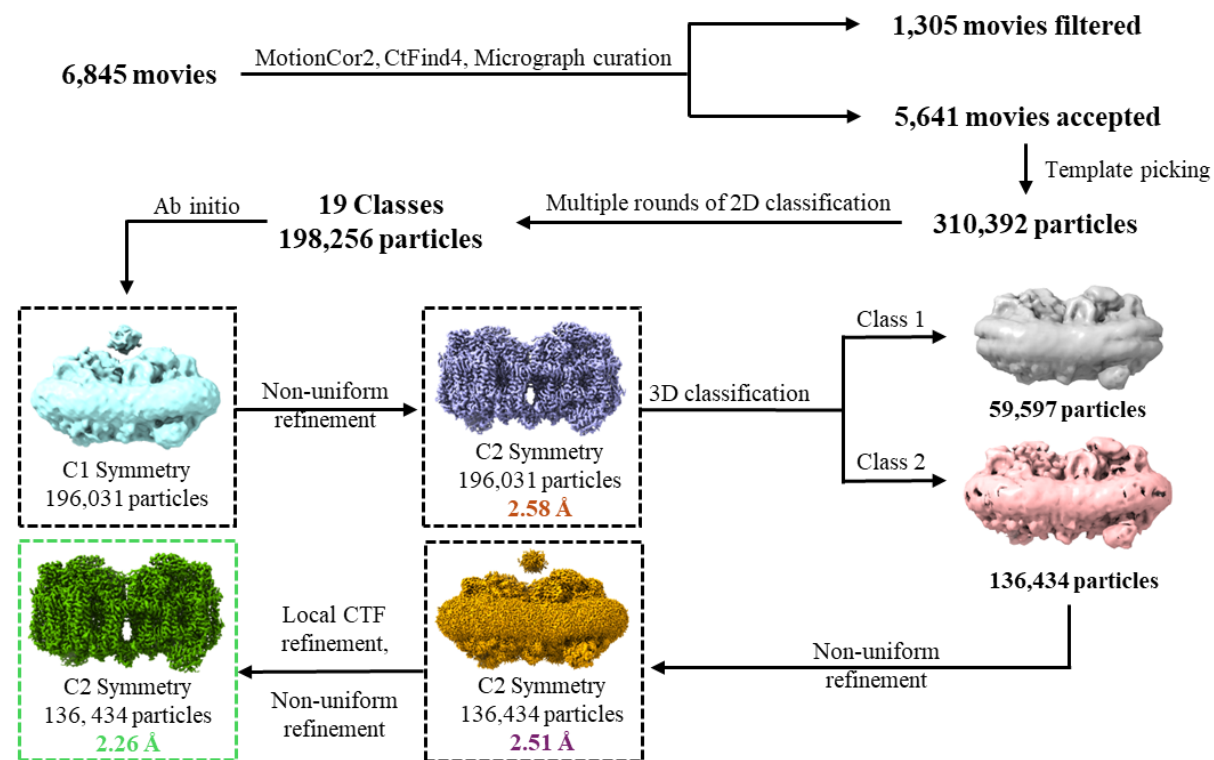
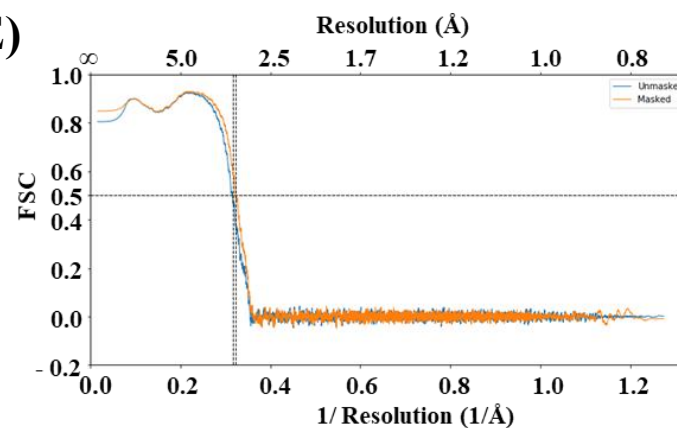
Supplementary Figure 5. Validation of the *Mab* QcrB mutants. (A) Respiratory profile of the *Mab* QcrB mutants were similar to *Mab* WT in the methylene blue assay confirming that the mutants did not alter the function of the *cyt-bcc:aa₃* oxidase. (B) Real-time monitoring of respiration in the presence of Q203 (100 nM, Black circle; 5 μ M, Orange square), Q203 (grey triangle) and DMSO (Green triangle) using Seahorse XFe96 Extracellular flux analyzer in *Mab* D311E/L314A QcrB mutant. (C) Real-time monitoring of respiration in the presence of Q203 (100 nM, Blue square) and DMSO (Grey circle) using Seahorse XFe96 Extracellular flux analyzer in *M. bovis* BCG. (D) Real-time monitoring of respiration in the presence of Q203 (100 nM, Black circle; 5 μ M, Orange square), Q203 (grey triangle) and DMSO (Green triangle) using Seahorse XFe96 Extracellular flux analyzer in *Mab* WT. (E) Real-time monitoring of respiration in the presence of Q203 (100 nM, Black circle; 5 μ M, Orange square), Q203 (grey triangle) and DMSO (Green triangle) using Seahorse XFe96 Extracellular flux analyzer in *Mab* D311E/L314I QcrB mutant.

			*		*		
<i>M. tuberculosis</i>	313	T	E	G	L	A	R 318
<i>M. smegmatis</i>	308	T	D	G	L	I	R 313
<i>M. abscessus subsp abscessus</i>	310	T	D	G	L	L	R 315
<i>M. abscessus subsp bolletii</i>	293	T	D	G	L	L	R 298
<i>M. abscessus subsp massiliense</i>	302	T	D	G	L	L	R 307
<i>M. avium</i>	323	T	E	G	L	A	R 328
<i>M. marinum</i>	323	T	E	G	L	A	R 328
<i>M. fortuitum</i>	308	T	E	G	L	A	R 313
<i>M. peregrinum</i>	308	T	E	G	L	A	R 313
<i>M. kansasii</i>	313	T	E	G	L	A	R 318
<i>M. intracellulare</i>	308	T	E	G	L	A	R 313
<i>M. chelonae</i>	318	T	E	G	L	A	R 323
<i>M. leprae</i>	312	T	E	G	L	A	R 317

Supplementary Figure 6. QcrB cavity region sequence alignment between mycobacterial species

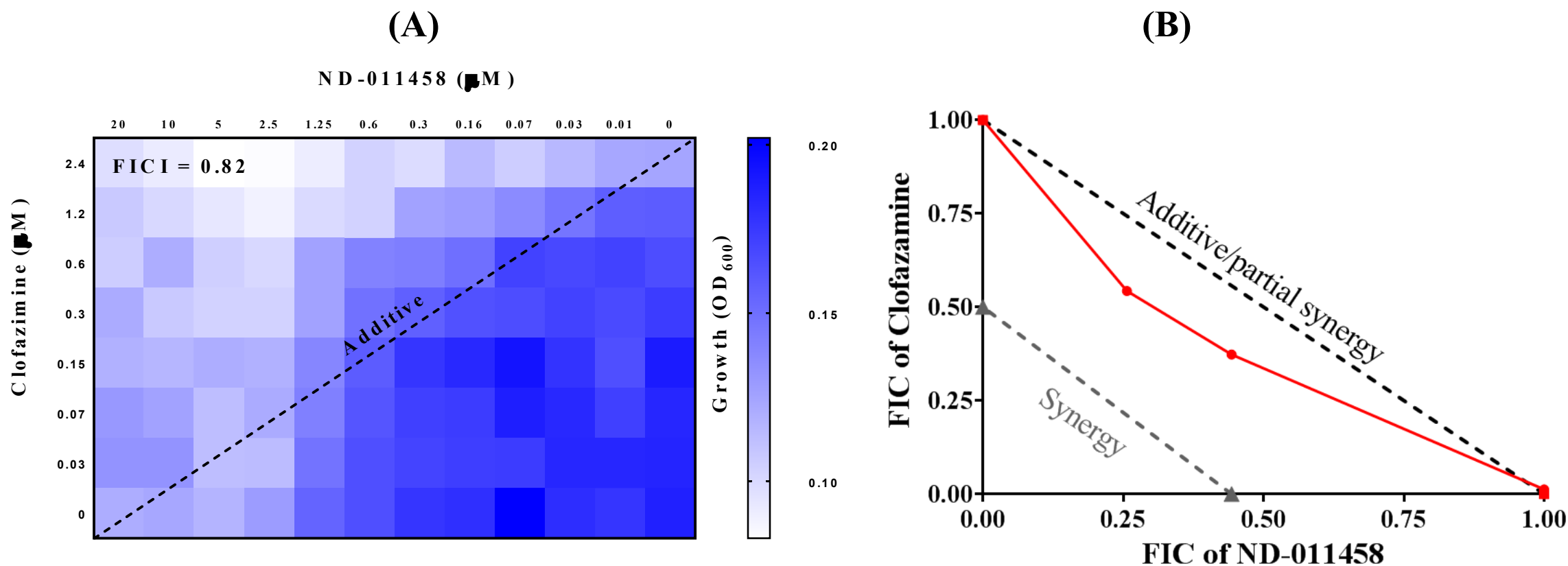


Supplementary Figure 7. Growth inhibitory activity of ND-011458 (Red circle), Q203 (Grey triangle) and Bedaquiline (BDQ, Black square) in (A) *M. abscessus* wild-type and (B) *M. abscessus* Δ*cydABDC*. The putative *cyt-bcc:aa₃* inhibitor ND-011458 achieves partial growth inhibition in comparison to the Bedaquiline in *M. abscessus* wild-type achieving an effect similar to a *cyt-bcc:aa₃* genetic knockout. The absence of complete growth inhibition in the wild-type is attributed to *cyt-bd*, encoded by *cydABDC*, which rescues respiration and growth. In the Δ*cydABDC* strain, although ND-011458 displays a steeper dose-response curve, complete growth inhibition could not be achieved proving the need for further chemical optimization.

(A)**(C)****(D)****(B)****(E)**

*Figure legend in next page

Supplementary Figure 8. Inhibitor-Enzyme Complex structure determination. (A) 2D-classification of picked particles in CryoSPARC. (B) Cryo-EM data processing workflow. The data processing pipeline was performed in cryoSPARC v3.3.1. 6,845 movies were collected and subjected to motion correction (MotionCor2) and CTF estimation (CtFind4). The processed micrographs were subsequently curated with the following thresholds: CTF fit resolution Min: 3.597 Å; Max: 7 Å and Astigmatism Min: 0.47 Å; Max: 500 Å resulting in the acceptance of 5,641 exposures for downstream processing. The *M. smegmatis* cyt-*bcc:aa*₃ oxidase structure (PDB: 6ADQ) was imported into cryoSPARC and used to generate templates for template-based picking yielding 310,392 particles. The particles were binned by a factor of 4 during the particle extraction process to reduce computational time and subjected to multiple rounds of 2D classification. 19 classes containing 198,256 particles were selected to construct an ab initio model with C1 symmetry. The ab initio model accepted 196,031 particles which were then reextracted at full resolution and subjected to non-uniform refinement resulting in a refined map with an overall resolution of 2.58 Å. A 3D classification job was performed to classify the particle into 2 classes using C1 symmetry. Class 1 emerged as the largest class with 136,434 particles which was then subjected to non-uniform refinement. The resulting map, which had an overall resolution of 2.51 Å, was refined further using local CTF refinement and another round of non-uniform refinement yielding a final cryo-EM map with an overall resolution of 2.26 Å with 136,434 particles. (C) Data processing in CryoSPARC resulted in a *M. abscessus* cyt-*bcc:aa*₃ structure at 2.26 Å. (D) Local resolution gradient map (1.75 Å, Blue; 3 Å, Red) reveals high resolution in core and key reaction centers. (E) Map vs Model FSC curve.



Supplementary Figure 9. Checkerboard Assessment of ND-011458 and Clofazimine (CFZ) combination. (A) Checkerboard assay heat map. (B) Isobolograms of the combination of ND-011458 and CFZ against *M. abscessus* CIP104536^T. The grey dash line indicates ideal isobole, where drugs act in synergy and independently while the black dash line indicates additive and partial synergy. An FICI of ≤ 0.5 indicates synergy, a FICI of >0.5 to 4 indicates additivity (no interaction), and an FICI of >4 indicates antagonism. The ND-011458 and CFZ combination is additive with a FICI of 0.82.

Supplementary Table 1 MALDI TOF data of band labelled QcrA in Figure 1B inset

Protein Name		Species		Accession No.		Protein MW				
Ubiquinol-cytochrome c reductase iron-sulfur subunit (Rieske iron-sulfur protein)		<i>Mycobacterium abscessus</i>		gi 169629054		43160.3				
Calc. Mass	Obsrv. Mass	± da	± ppm	Start seq.	End seq.	Sequence	ION score	C. I. %	Modification	Rank Result Type
816.425	816.4337	0.0087	11	44	50	WPVEGTK				Mascot
842.4916	842.5078	0.0162	19	280	286	NPVMLIR				Mascot
858.4866	858.4999	0.0133	15	280	286	NPVMLIR			Oxidation (M)[4]	Mascot
858.4866	858.4999	0.0133	15	280	286	NPVMLIR			Oxidation (M)[4]	Mascot
943.5029	943.5165	0.0136	14	287	294	VRPTDMPK				Mascot
959.4979	959.5128	0.0149	16	287	294	VRPTDMPK			Oxidation (M)[6]	Mascot
1054.5826	1054.6005	0.0179	17	271	279	LSHIQMGIR				Mascot
1070.5775	1070.5924	0.0149	14	271	279	LSHIQMGIR			Oxidation (M)[6]	Mascot
1208.6058	1208.626	0.0202	17	218	227	YHGETIYLGR	74	99.708		Mascot
1208.6058	1208.626	0.0202	17	218	227	YHGETIYLGR				Mascot
1267.6025	1267.623	0.0205	16	135	146	HDGPGSAEVDRK				Mascot
1345.7111	1345.7303	0.0192	14	124	134	FIPQEISIQDR				Mascot
1345.7111	1345.7303	0.0192	14	124	134	FIPQEISIQDR				Mascot
1354.7478	1354.766	0.0182	13	206	217	QPVLLTSGWTPR	55	77.247		Mascot
1354.7478	1354.766	0.0182	13	206	217	QPVLLTSGWTPR				Mascot
1448.7744	1448.7878	0.0134	9	28	40	LGTNLDGVEIVYR				Mascot
1473.806	1473.8214	0.0154	10	123	134	KFIPQEISIQDR				Mascot
1766.802	1766.8132	0.0112	6	300	314	GQENFNYGDLFAYTK				Mascot

1830.9708	1830.9923	0.0215	12	28	43	LGTNLDGVEIVYREPR	88	99.987	Mascot
1830.9708	1830.9923	0.0215	12	28	43	LGTNLDGVEIVYREPR			Mascot
1872.0073	1872.0194	0.0121	6	147	163	TIVAQLQDTLDTSTLPR	99	100	Mascot
1872.0073	1872.0194	0.0121	6	147	163	TIVAQLQDTLDTSTLPR			
1894.897	1894.9243	0.0273	14	299	314	KGQENFNYGDLFAYTK			Mascot
2089.0171	2089.0425	0.0254	12	239	256	IRPEDIDAGGMETVFPWR			Mascot
2105.012	2105.0291	0.0171	8	239	256	IRPEDIDAGGMETVFPWR		Oxidation (M)[11]	Mascot
2830.3774	2830.4028	0.0254	9	2	27	SVSDADKPEIPSDEQLAAMSRDELVK	68	98.836	Mascot
2830.3774	2830.4028	0.0254	9	2	27	SVSDADKPEIPSDEQLAAMSRDELVK			Mascot
2846.3723	2846.3831	0.0108	4	2	27	SVSDADKPEIPSDEQLAAMSRDELVK		Oxidation (M)[19]	Mascot
3487.7896	3487.833	0.0434	12	358	389	ALAQLPLTVDKDGYLVANGDFVEPVGPAPWER			Mascot

Supplementary Table 2 MALDI TOF data of band labelled QcrB in Figure 1B inset

Protein Name		Species		Accession No.		Protein MW				
Ubiquinol-cytochrome c reductase cytochrome b subunit		<i>Mycobacterium abscessus</i>		gi 169629053		60416.4				
Calc. Mass	Obsrv. Mass	± da	± ppm	Start seq.	End seq.	Sequence	ION score	C. I. %	Modification	Rank Result Type
843.4835	843.4924	0.0089	11	431	437	WAIGLQR				Mascot
843.4835	843.4924	0.0089	11	431	437	WAIGLQR				Mascot
890.4553	890.4558	0.0005	1	22	29	YHLAAGMK				Mascot
900.5916	900.5916	0	0	255	262	ILPVFALK				Mascot
906.4501	906.4534	0.0033	4	22	29	YHLAAGMK			Oxidation (M)[7]	Mascot
923.3887	923.4036	0.0149	16	14	21	QAEAMDSR			Oxidation (M)[5]	Mascot
958.5145	958.5239	0.0094	10	129	136	IFFTGAFR				Mascot
989.501	989.513	0.012	12	2	10	SDTAQKPSR				Mascot
1269.6222	1269.6262	0.004	3	237	248	HTQFPGPATEK				Mascot
1379.7893	1379.79	0.0007	1	441	453	AVLEHGIETGIK	65	98.939		Mascot
1379.7893	1379.79	0.0007	1	441	453	AVLEHGIETGIK				Mascot
1535.8904	1535.8982	0.0078	5	441	454	AVLEHGIETGIKR				Mascot
1542.7799	1542.7881	0.0082	5	90	102	AYETTLNISFEVR				Mascot
1737.9493	1737.9561	0.0068	4	438	453	SDRAVLEHGIETGIK				Mascot
1742.9045	1742.9095	0.005	3	356	370	LTGDDAHHNLLQRPR	8	0		Mascot
1742.9045	1742.9095	0.005	3	356	370	LTGDDAHHNLLQRPR				Mascot
1870.9995	1870.9784	-0.0211	-11	355	370	KLTGDDAHHNLLQRPR				Mascot
2173.0957	2172.988	-0.1077	-50	84	102	GVQMSKAYETTLNISFEVR				Mascot
2321.1616	2321.012	-0.1496	-64	109	128	QIHHWAALMFAASIMVHMAR				Mascot
3468.6204	3468.5889	-0.0315	-9	493	526	LGSAGAPGTGSFLFADPADEQHALAEAEHEAHHK				Mascot
3867.9565	3867.9355	-0.021	-5	455	489	LPHGEYIEIHQPLAGVDEHGHAIPLEYQGAPVPQR				Mascot
3867.9565	3867.9355	-0.021	-5	455	489	LPHGEYIEIHQPLAGVDEHGHAIPLEYQGAPVPQR				Mascot

Supplementary Table 3 MALDI TOF data of band labelled QcrC in Figure 1B inset

Protein Name		Species		Accession No.		Protein MW				
Ubiquinol-cytochrome c reductase cytochrome c subunit		<i>Mycobacterium abscessus</i>		gi169629055		31350.9				
Calc. Mass	Obsrv. Mass	± da	± ppm	Start seq.	End seq.	Sequence	ION score	C. I. %	Modification	Rank Result Type
816.3958	816.4096	0.0138	17	128	134	NEAQAQR				Mascot
816.3958	816.4096	0.0138	17	128	134	NEAQAQR				Mascot
849.4828	849.5032	0.0204	24	245	251	DIIAYVR				Mascot
977.5778	977.603	0.0252	26	244	251	KDIIAYVR	19	0		Mascot
977.5778	977.603	0.0252	26	244	251	KDIIAYVR				Mascot
1045.5272	1045.5522	0.025	24	165	174	DGAVAQESLR				Mascot
1316.6553	1316.6774	0.0221	17	163	174	DRDGAVAQESLR	31	0		Mascot
1316.6553	1316.6774	0.0221	17	163	174	DRDGAVAQESLR				Mascot
1436.6158	1436.6462	0.0304	21	187	198	LNCASCHNFTGR			Carbamidomethyl (C)[3,6]	Mascot
1791.0011	1791.0259	0.0248	14	237	251	QLTVDEKKDIIAYVR	36	0		Mascot
1791.0011	1791.0259	0.0248	14	237	251	QLTVDEKKDIIAYVR				Mascot
2008.0498	2008.0725	0.0227	11	103	122	GPSLIGVGAAVYFQVSTGR				Mascot
2874.3904	2874.4258	0.0354	12	136	162	DPIFDEEQTDALGAYIQANGGGPQVIR				Mascot
2907.3904	2907.4265	0.0361	12	207	232	FAPELDPATEQQIYTAML TGPQNMPK			Oxidation (M)[17]	Mascot
2923.3853	2923.4077	0.0224	8	207	232	FAPELDPATEQQIYTAML TGPQNMPK			Oxidation (M)[17,24]	Mascot
3002.4854	3002.5254	0.04	13	135	162	KDPIFDEEQTDALGAYIQANGGGPQVIR	50	20.253		Mascot
3002.4854	3002.5254	0.04	13	135	162	KDPIFDEEQTDALGAYIQANGGGPQVIR				Mascot

Supplementary Table 4 MALDI TOF data of band labelled SOD in Figure 1B inset

Protein Name		Species		Accession No.		Protein MW				
Superoxide dismutase [Cu-Zn] precursor		<i>Mycobacterium abscessus</i>		gi 169631262		23974.9				
Calc. Mass	Obsrv. Mass	± da	± ppm	Start seq.	End seq.	Sequence	ION score	C. I. %	Modification	Rank Result Type
875.4291	875.4757	0.0466	53	230	238	VACGLIDAG			Carbamidomethyl (C)[3]	Mascot
1233.5858	1233.5951	0.0093	8	196	206	SDNFANIPAER	28	0		Mascot
1233.5858	1233.5951	0.0093	8	196	206	SDNFANIPAER				Mascot
1590.854	1590.8483	-0.0057	-4	106	119	LTPGFHGLHIHSFK				Mascot
2070.0291	2070.0217	-0.0074	-4	76	95	LADGTPVATAAFVFQDGYAR	154	100		Mascot
2070.0291	2070.0217	-0.0074	-4	76	95	LADGTPVATAAFVFQDGYAR				Mascot
3202.6113	3202.5581	-0.0532	-17	165	195	DGSGELVTTADSFTKEDLLAGNGTAMIIHEK				Mascot

Supplementary Table 5 MALDI TOF data of band labelled LpqE in Figure 1B inset

Protein Name		Species		Accession No.		Protein MW				
Putative lipoprotein lpqE precursor		Mycobacterium abscessus		gi 169627670		23258.9				
Calc. Mass	Obsrv. Mass	± da	± ppm	Start seq.	End seq.	Sequence	ION score	C. I. %	Modification	Rank Result Type
919.4559	919.4667	0.0108	12	189	195	FTFTFEK	68	98.698		Mascot
919.4559	919.4667	0.0108	12	189	195	FTFTFEK				Mascot
1023.5105	1023.5231	0.0126	12	180	188	DLADGLTYR	44	0		Mascot
1023.5105	1023.5231	0.0126	12	180	188	DLADGLTYR				Mascot
1292.6957	1292.7034	0.0077	6	58	69	NIHLVGNSDPVK	47	0		Mascot
1292.6957	1292.7034	0.0077	6	58	69	NIHLVGNSDPVK				Mascot
1388.7017	1388.7141	0.0124	9	105	118	VTLSGSDIPATGR	54	68.043		Mascot
1388.7017	1388.7141	0.0124	9	105	118	VTLSGSDIPATGR				Mascot
1430.6044	1430.6136	0.0092	6	214	227	QHTIDGGGHEGGEH				Mascot
1576.8553	1576.8712	0.0159	10	58	71	NIHLVGNSDPVKQR	105	100		Mascot
1576.8553	1576.8712	0.0159	10	58	71	NIHLVGNSDPVKQR				Mascot
1629.8119	1629.8113	-0.0006	0	119	134	LFVGS AEGQEPPAEAK	44	0		Mascot
1629.8119	1629.8113	-0.0006	0	119	134	LFVGS AEGQEPPAEAK				Mascot
1733.9181	1733.9373	0.0192	11	196	213	AGEVTVAVPIDAGPNAPR	140	100		Mascot
1733.9181	1733.9373	0.0192	11	196	213	AGEVTVAVPIDAGPNAPR				Mascot
1786.9432	1786.9346	-0.0086	-5	76	92	AELVL VIANESADISDK				
2630.3518	2630.3506	-0.0012	0	93	118	LTSITSPDEIGKVTLSGSDIPATGR				
3028.5935	3028.5945	0.001	0	76	104	AELVL VIANESADISDKLTSITSPDEIGK	30	0		
3028.5935	3028.5945	0.001	0	76	104	AELVL VIANESADISDKLTSITSPDEIGK				Mascot

Supplementary Table 6 Cryo-EM data acquisition and Cryo-EM map statistics of the resolved inhibitor-free and ND-011458-bound *Mab* cyt-*bcc:aa*₃

Data collection	Inhibitor-free	ND-011458-bound
Electron Microscope	Titan Krios	Titan Krios
Camera	Gatan K3	Falcon 4i
Mode	Super-resolution counting	Super-resolution counting
Voltage (kV)	300	300
Nominal Magnification	130,000 ×	165, 000 x
Calibrated physical pixel size (Å)	0.671	0.76
Exposure time (s)	2.83	2.83
Total exposure (e ⁻ /Å ²)	56	60
Number of frames	40	40
Defocus range (μM)	-0.7 to -2.0	-0.5 to -1.5
Cryo-EM map statistics		
Number of micrographs	5,541	5,641
Number of particle images selected (after auto-pick)	956,580	310,392
Number of particle images after clean-up (after 2D classification)	334,881	198,256
Particle images contributing to maps	137,735	135,891
Applies symmetry	C2	C2
Applied Box size (pix)	600	600
Applied B-factor (Å ²)	-92.7	-52.1
Global resolution (FSC = 0.143, Å)	2.66	2.26

Supplementary Table 7 Model building, model refinement and model statistics for the Inhibitor-free and ND-011458-bound *Mab cyt-bcc:aa₃*

EM model	Inhibitor-free	ND-011458-bound
Modelling software	Coot	Coot
Refinement software	Phenix	Phenix
MolProbity score	1.72 (89 th Percentile)	1.57 (93 rd Percentile)
EMRinger score	4.21	4.58
Number of residues (protein)	5612	5614
Clash score	6.74 (88 th Percentile)	4.32 (96 th Percentile)
CC (Mask)	0.83	0.84
RMS bond length (Å)	0.008	0.004
RMS bond angle (°)	1.076	0.655
Ramachandran favoured (%)	95.04	95.66
Ramachandran outliers (%)	0.05	0.11
Rama-Z	0.33 ± 0.11	1.21 ± 0.11
Ligands	9 XX: 4, 9Y0: 6, 9YF: 8, FES: 2, HEC: 4, HEA: 4, MQ9: 10, HEM: 4, PLM: 4, CU: 8, OXY:2, H ₂ O: 74	9 XX: 4, 9Y0: 6, 9YF: 8, FES: 2, HEC: 4, HEA: 4, MQ9: 10, HEM: 4, PLM: 4, CU: 8, OXY:2, LIG: 2, H ₂ O:74

Supplementary Table 8 Forward and reverse primer sequences for generating mutants

Construct	Oligonucleotide Sequence (5'– 3')
<i>Mab</i> QcrB F158Y (Forward primer)	GAA GGT T <u>A</u> C TTC GGA TAC TCC CTG CCC
<i>Mab</i> QcrB F158Y (Reverse primer)	TCC GAA G <u>T</u> A ACC TTC GAA CAT CGC CAG
<i>Mab</i> QcrB D311E (Forward primer)	TGG ACC GA <u>A</u> GGC CTG CTG CGC ATC ATC
<i>Mab</i> QcrB D311E (Reverse primer)	CAG GCC <u>T</u> TC GGT CCA CAT CAT GTA GAA GTC
<i>Mab</i> QcrB D311E/L314I (Forward primer)	C CTG ATC CGC <u>A</u> T <u>C</u> ATC CCG GCT TGG
<i>Mab</i> QcrB D311E/L314I (Reverse primer)	T GAT GCG <u>G</u> A <u>T</u> CAG GCC <u>T</u> TC GGT CCA
<i>Mab</i> QcrB L314A (Forward primer)	GC CTG <u>G</u> C <u>G</u> CGC ATC ATC CCG G
<i>Mab</i> QcrB L314A (Reverse primer)	G <u>C</u> G <u>C</u> CAG GCC GTC GGT CCA C
<i>Mab</i> QcrB D311E/L314A (Forward primer)	GAC CGA <u>A</u> GG CCT <u>G</u> G <u>C</u> GCG CAT CAT C
<i>Mab</i> QcrB D311E/L314A (Reverse primer)	CAG GCC <u>T</u> TC GGT CCA CAT CAT GTA GAA GTC
<i>Mab</i> QcrB G179S (Forward primer)	GCT TTC C <u>A</u> G CAT CAC CAT GGG CCT TCC
<i>Mab</i> QcrB G179S (Reverse primer)	GTG ATG C <u>T</u> G GAA AGC GCC GCG CG
<i>Mab</i> QcrB C393A (Forward primer)	<u>G</u> C <u>T</u> ATG AAC GAC ATC ATC GCG CTG AAG TTC
<i>Mab</i> QcrB C393A (Reverse primer)	TGA TGT CGT TCA TA <u>G</u> <u>C</u> CA TGA GCG TGA ACA

* Bold and underlined nucleotides are the nucleotide changed.

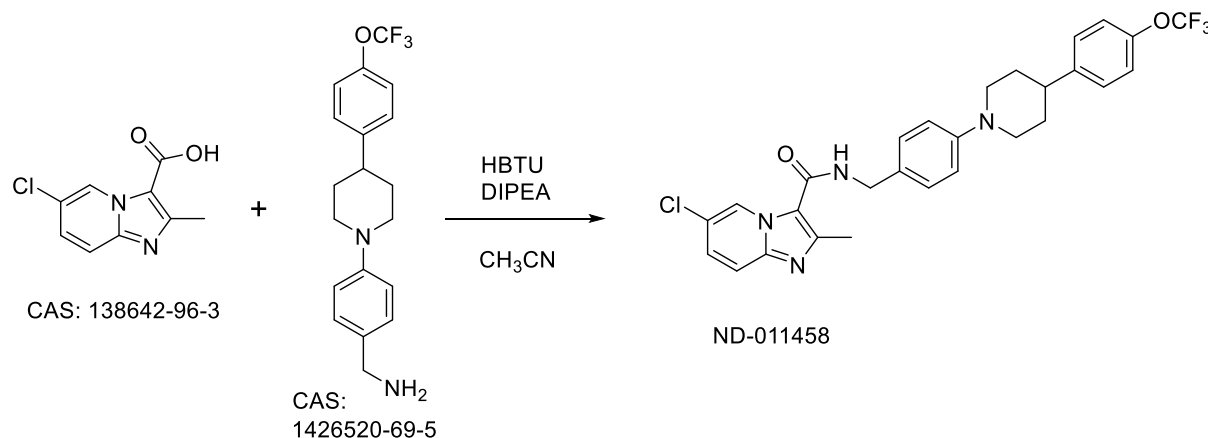
	MIC ₅₀ (nM)
<i>M. abscessus</i> subsp. <i>abscessus</i> (R)	539 ± 36
<i>M. abscessus</i> subsp. <i>abscessus</i> (S)	483 ± 34
<i>M. abscessus</i> subsp. <i>bolletii</i>	312 ± 64
<i>M. abscessus</i> subsp. <i>massiliense</i>	637 ± 76

Supplementary Table 9. Growth Inhibitory activity of ND-011458 against *Mab* complex. The MIC₅₀ values indicate the minimum drug concentration at which 50% of bacterial growth was inhibited. R: rough variant. S: smooth variant.

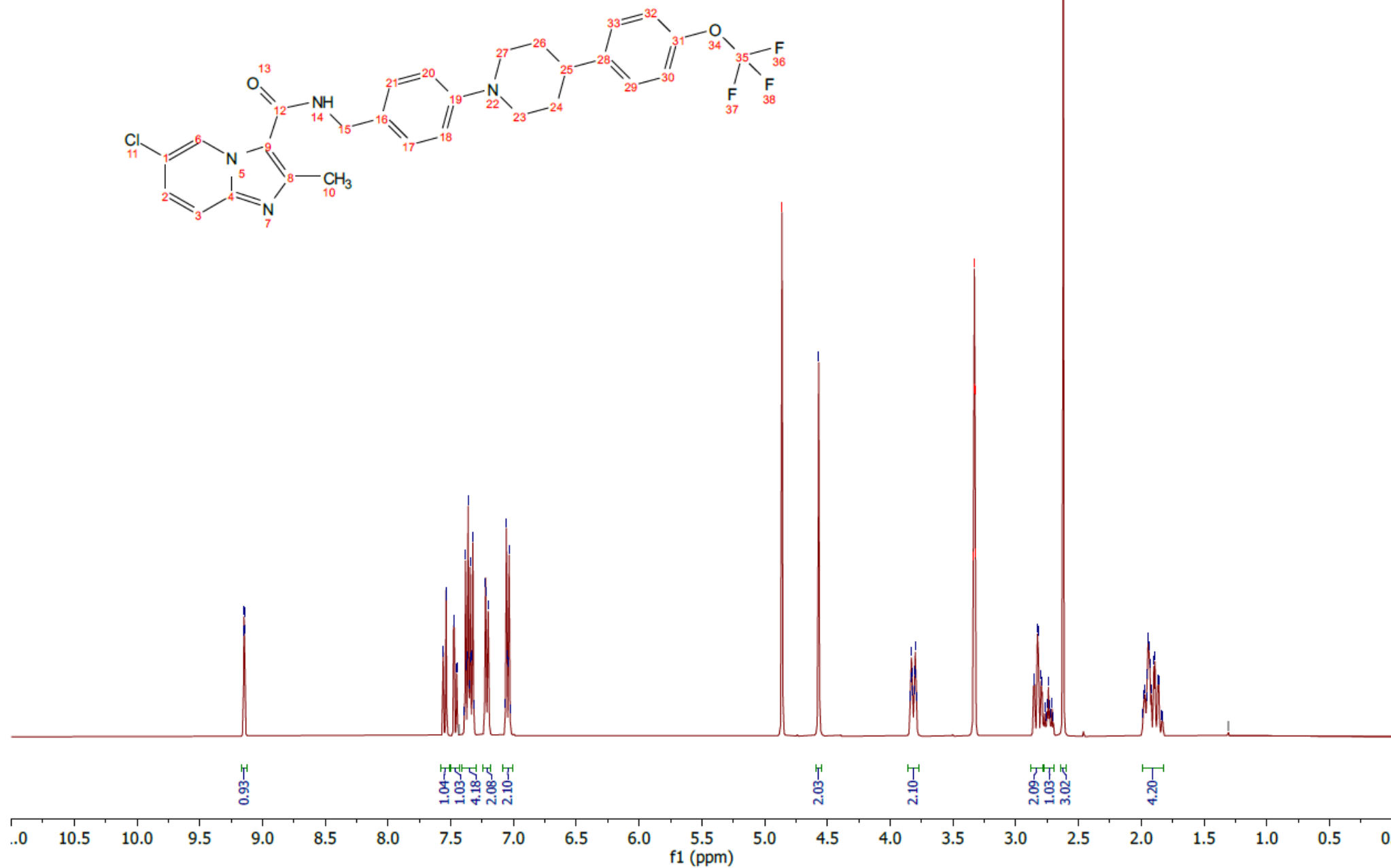
Drug A	Combination with drug B	MIC				FICI	Outcome
		Drug A	Drug A in combination	Drug B	Drug B in combination		
ND-011458	Clofazimine	0.97 μM	0.43 μM	1.64 μM	0.61 μM	0.82	Additive

Supplementary Table 10. The FICI was calculated as (MIC of drug A in combination/MIC of drug A alone) + (MIC of drug B in combination/MIC of drug B alone). An FICI of ≤ 0.5 indicates synergy, a FICI of > 0.5 to 4 indicates additivity (no interaction), and an FICI of > 4 indicates antagonism.

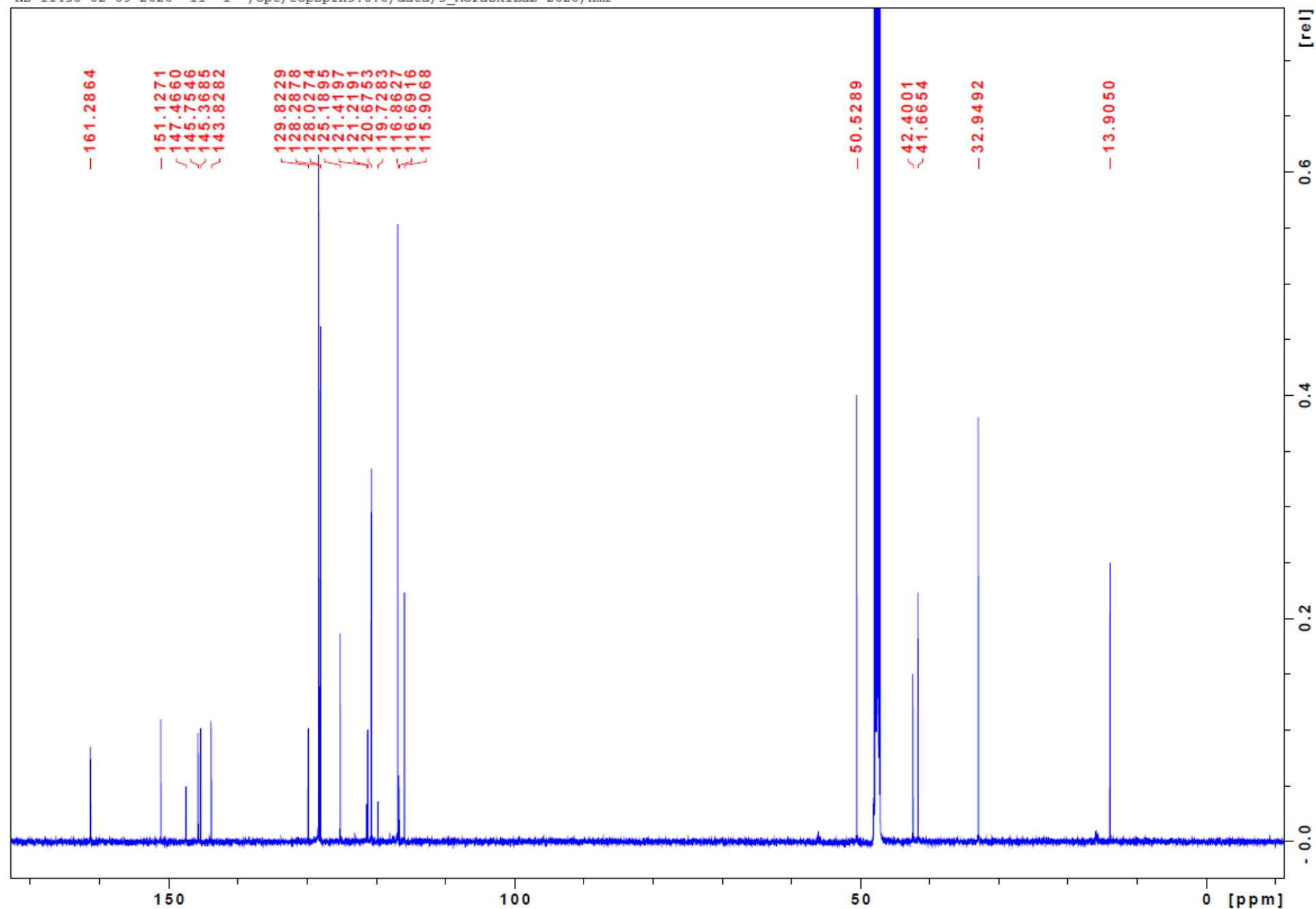
General synthesis routes to compounds



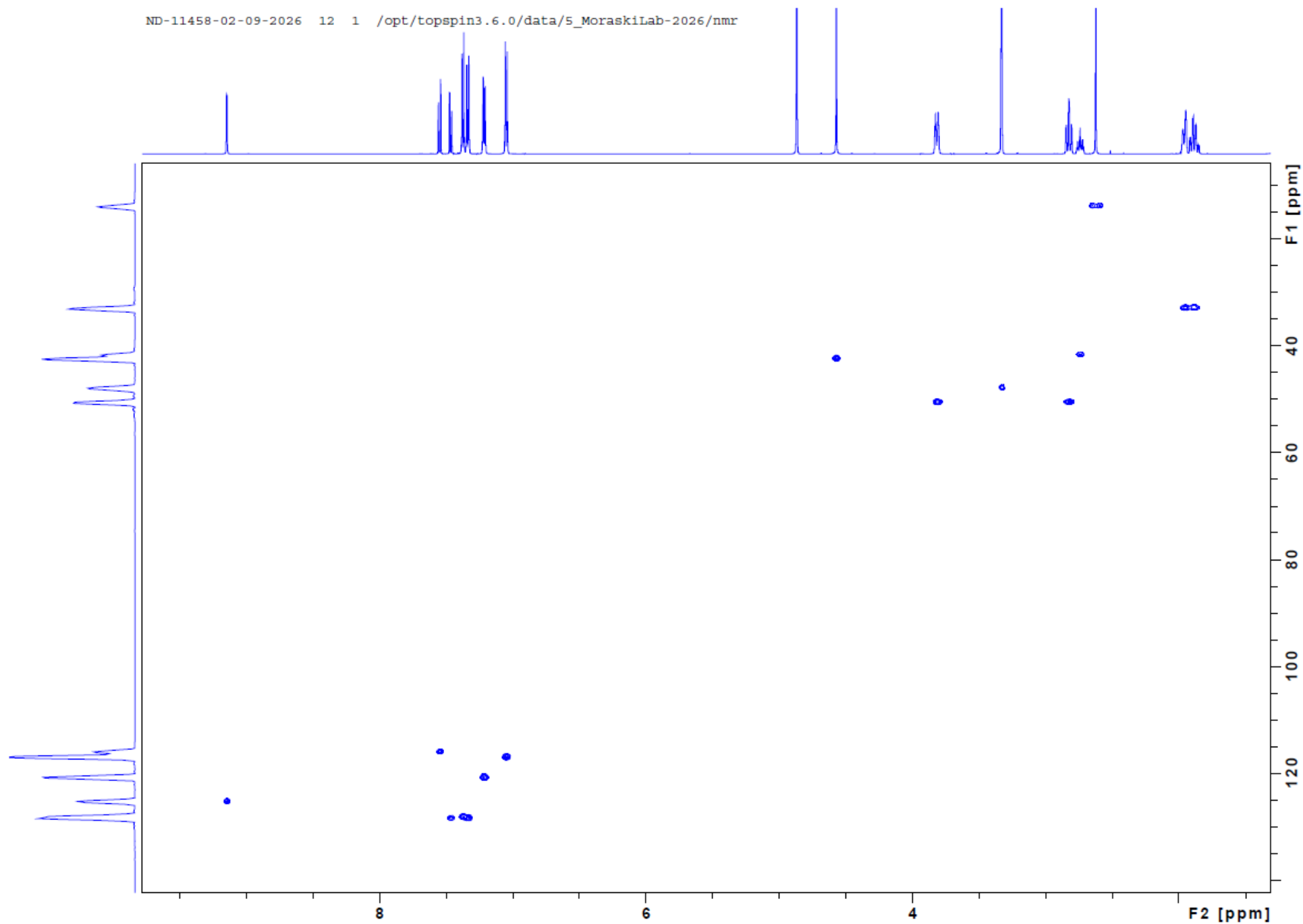
In a sealed reaction V-vial, 6-chloro-2-methylimidazo[1,2-*a*]pyridine-3-carboxylic acid (CAS: 138642-96-3, 0.06 g, 0.29 mmol) and (4-(4-(4-(trifluoromethoxy)phenyl)piperidin-1-yl)phenyl)methanamine (CAS: 1426520-69-5, 0.10 g, 0.29 mmol) were dissolved in 5 ml of CH₃CN. Then, 2-(1H-Benzotriazole-1-yl)-1,1,3,3-tetramethyluronium hexafluorophosphate (HBTU, 0.11 g, 0.29 mmol) and *N,N*-Diisopropylethylamine (DIPEA, 0.07 mL, 0.43 mmol) were added, and the reaction was sealed and stirred at RT overnight. At this time, the reaction mixture was concentrated to dryness. The residue was diluted with CH₂Cl₂, washed with 25% aqueous Na₂CO₃ solution (2x), water, and 5% acetic acid solution (2x). The organic phase was collected, dried over sodium sulfate (Na₂SO₄), filtered to remove the drying agent, and then concentrated in vacuo to dryness. The desired product was crystallized from hot isopropanol to give 6-chloro-2-methyl-*N*-(4-(4-(4-(trifluoromethoxy)phenyl)piperidin-1-yl)benzyl)imidazo[1,2-*a*]pyridine-3-carboxamide (ND-011458), an off-white solid (60 mg, 37%). ¹H NMR (400 MHz, MeOD) δ ppm 9.15 (d, *J* = 2.0 Hz, 1H), 7.56 (d, *J* = 9.5 Hz, 1H), 7.47 (dd, *J* = 9.5, 2.0 Hz, 1H), 7.42 – 7.30 (m, 4H), 7.22 (d, *J* = 8.2 Hz, 2H), 7.10 – 7.01 (m, 2H), 4.57 (s, 2H), 3.82 (dt, *J* = 13.1, 3.3 Hz, 2H), 2.89 – 2.81 (m, 1H), 2.85 – 2.78 (m, 1H), 2.75 (tt, *J* = 11.9, 3.8 Hz, 1H), 2.63 (s, 3H), 2.00 – 1.81 (m, 4H). ¹⁹F NMR (376 MHz, MeOD) δ -59.55, uncorrected. HRMS (EI), *M*+1 calcd. for C₂₈H₂₇ClF₃N₄O₂, 543.1775; found 543.1758, retention time = 5.066 min, 100% pure.



ND-11458-02-09-2026 11 1 /opt/topspin3.6.0/data/5_MoraskiLab-2026/nmr



ND-11458-02-09-2026 12 1 /opt/topspin3.6.0/data/5_MoraskiLab-2026/nmr



Target Screening Report



Agilent

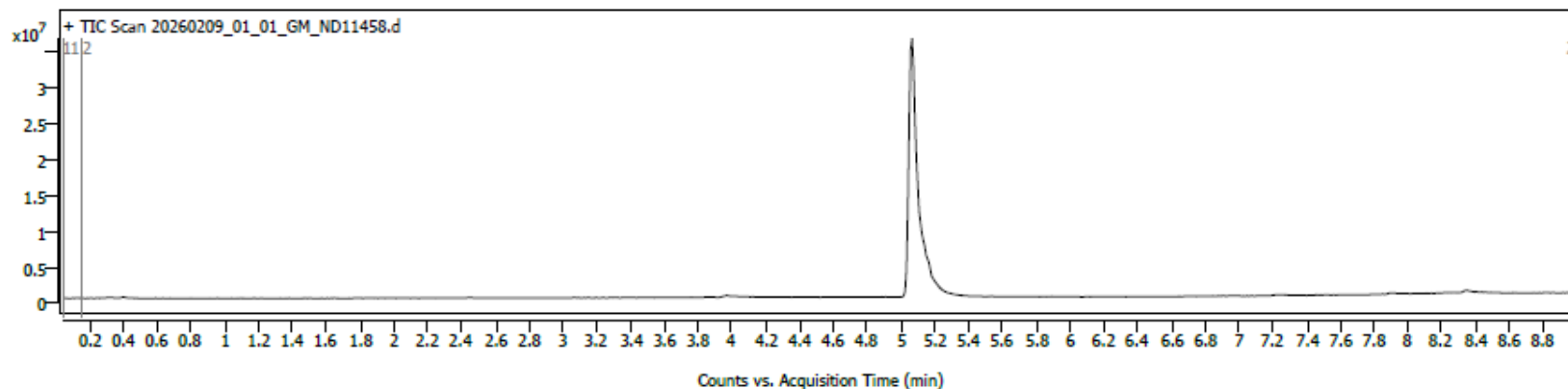
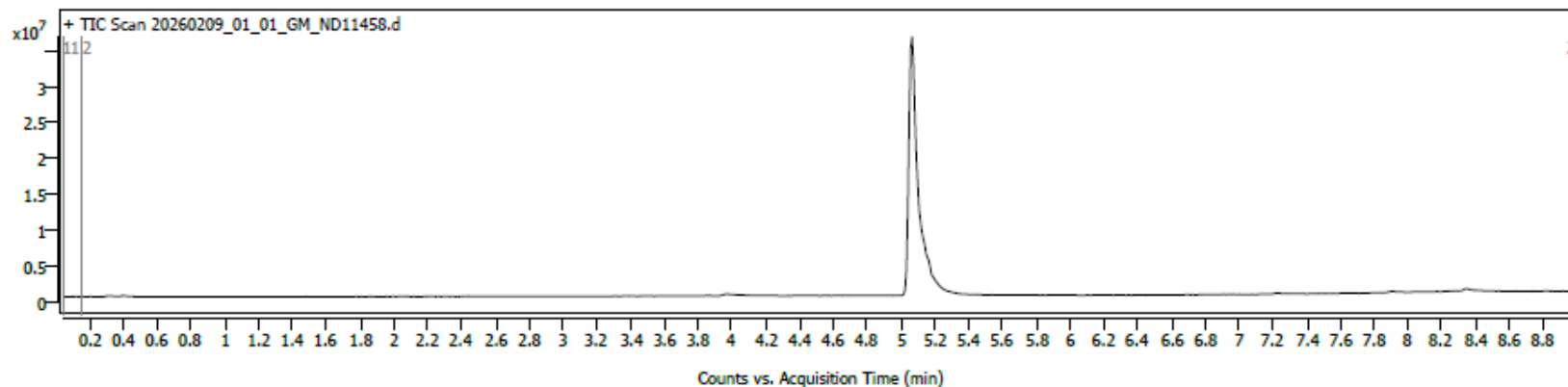
Trusted Answers

HRMS

Sample Information

Name		Data File Path	D:\MassHunter\Data\Facility\2026\20260203_KLM_VGK_MS_eclipse18-050\20260209_01_01_GM_ND11458.d
Sample ID		Acq. Time (Local)	2/9/2026 11:24:49 AM (UTC-07:00)
Instrument	Instrument 1	Method Path (Acq)	D:\MassHunter\Methods\Facility\EclipseC18-50\20241028_PLp_600uL_1minprerun_0-9min_2-98a1b1_pos1_50deg_UV1_2Hz_v01.m
MS Type	QTOF	Version (Acq SW)	6200 series TOF/6500 series Q-TOF 10.1 (48.0)
Inj. Vol. (ul)	3	IRM Status	Success
Position	P2-F1	Method Path (DA)	D:\MassHunter\Methods\10.0\TargetScreening_V2.m
Plate Pos.		Target Source Path	C28H26ClF3N4O2
Operator		Result Summary	1 qualified (1 targets)

Sample Chromatograms



Compound Summary

Cpd	Name	Formula	CAS	RT	Mass	Mass (Tgt)	Diff (Tgt, ppm)	Score	Algorithm
1		C28 H26 Cl F3 N4 O2		5.066	542.1687	542.1696	-1.67	89.75	FBF

Compound Summary

Cpd	Name	Formula	CAS	RT	Mass	Mass (Tgt)	Diff (Tgt, ppm)	Score	Algorithm
1		C28 H26 Cl F3 N4 O2		5.066	542.1687	542.1696	-1.67	89.75	FBF

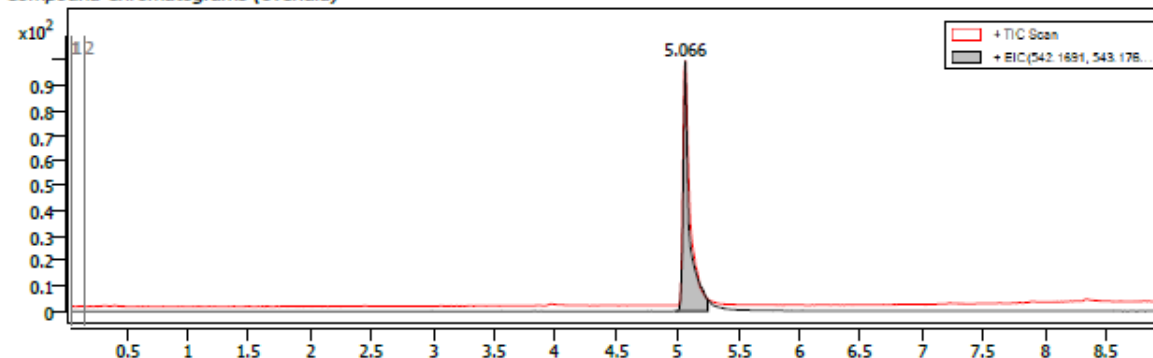
Compound Details

Cpd. 1: C28 H26 Cl F3 N4 O2

Name	Formula	RT	RI	Mass Diff (Tgt, ppm)	CAS	ID Source	Score	Algorithm
	C28 H26 Cl F3 N4 O2	5.066		542.1687	-1.67	FBF	89.75	FBF

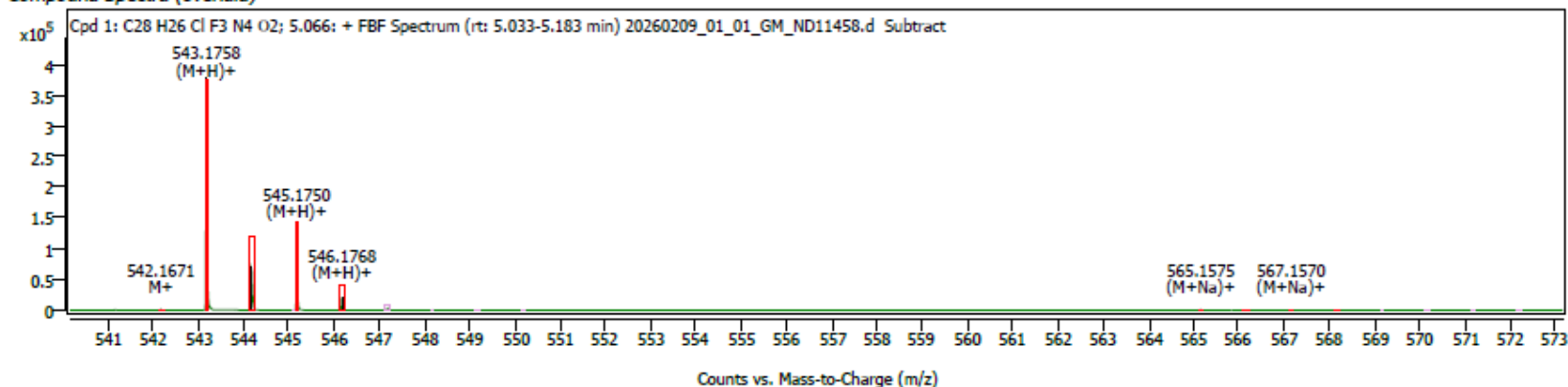
Species	m/z	Score (Tgt)	Score (Lib)	Score (DB)	Score (MFG)	Score (RT)
M+ (M+H)+	542.1671	543.1758	89.75			
(M+Na)+	565.1575					

Compound Chromatograms (overlaid)



Structure

Compound Spectra (overlaid)



Compound ID Table

Name	Formula	Species	RT	RT Diff	Mass	CAS	ID Source	Score	Score (Lib)	Score (Tgt)
	C28 H26 Cl F3 N4 O2	M+ (M+H)+ (M+Na)+	5.066		542.1687		FBF	89.75		89.75